Int. J. Heat Mass Transfer. Vol. 21, pp. 341–349. Pergamon Press 1978. Printed in Great Britain

THE MELTING OF METAL SPHERES INVOLVING THE INITIALLY FROZEN SHELLS WITH DIFFERENT MATERIAL PROPERTIES

OLAF EHRICH,* YUN-KEN CHUANG† and KLAUS SCHWERDTFEGER*

(*Received* 23 *December* 1976)

Abstract—The method of the Green's function has been used for numerical calculation of the melting rate of sponge metal spheres. This problem is of interest for new industrial processes, e.g. for the melting of sponge iron pellets. After immersion into the liquid metal the shell freezes around the sphere initially. The shell is dense and has different material properties than the porous region. The starting equation is Fourier's second law with the corresponding initial and boundary conditions. It is shown that by the use of the Green's function the partial differential equation for heat flow for the two domains can be transformed to integral equations containing only the temperature and temperature gradients at the surface of the domain, and that by this measure the numerical effort is reduced considerably. The same calculations are carried out for the simpler problem that the sphere and the initially frozen shell have the same material properties. In this case dimensionless total melting time is a function of only two other dimensionless quantities, and the computed functional relationship is given for the range of interest for practical application.

NOMENCLATURE

- c, specific heat per mass unit;
- h, heat-transfer coefficient for transport of heat from the melt to the solid surface;
- l, number specifying node on s scale;
- n, number specifying node on time scale;
- p, dimensionless time;
- r, radial coordinate;
- s, dimensionless radial coordinate;
- t, time;
- t_a, time at which shell disappears;
- Bi, Biot number;
- Bi', modified Biot number $BiU_{\delta m}$;
- G, Green's function;
- ΔH, heat of fusion of metal per mass unit;
- Ph, dimensionless heat of fusion;
- R, radius of sphere at time t;
- R_0, radius of sphere at time $t = 0$;
- R_{max}, maximum radius of sphere;
- S, dimensionless radius of sphere;
- T, temperature;
- T_{0s}, temperature of solid sphere at $t = 0$;
- T_{0m}, temperature of the infinite medium of melt;
- T_f, melting temperature of metal;
- T_a, temperature at radial position at time t_a;
- U, dimensionless temperature.

Greek symbols

- α, thermal diffusivity ($= \lambda/\rho c$);
- β, constant which is either 1 or α_{II}/α_I depending on the domain (I or II) to which equation (10) is applied;
- δ, Dirac delta function, $\delta(q) = 0$ for $q \neq 0$, $\int_{-\infty}^{\infty} \delta(q)\,dq = 1$;
- λ, heat conductivity;
- ρ, density;
- ξ, radial dimensionless coordinate at which heat source is liberated at $t = \tau$;
- τ, dimensionless time at which heat source is liberated at $s = \xi$.

IN THE present paper the melting of a metal sphere involving the initially frozen shell with different material properties will be investigated. This problem is of interest for new industrial processes in which porous metal pieces are melted in their own melt (e.g. melting of sponge iron pellets) or in which the metal pieces are submersed into hot slag for melting. A shell with different material properties will freeze initially at the periphery of the sphere. The shell will grow to a certain thickness, it will then remelt, finally the original sphere will melt. Growth and remelting of the shell is controlled by heat conduction in both domains, and two equations for heat conduction have to be solved simultaneously in the computations.

Although the above problem has not been treated previously in the literature, papers are available [1–7] dealing with closely related spherical heat conduction problems, e.g. with the melting of dense spheres [1, 2], with outward and inward spherical solidification [3–6] or with the formation and dissolution of a slag crust on a metal sphere [7]. Apart from certain limiting cases [8] for which exact analytical solutions can be derived, the solutions obtained involve approximate analytical (e.g. perturbation method) or numerical procedures.

In the present paper the melting problem described above has been analysed by using the Green's function technique which has been used previously [9–11] on

*Max-Planck-Institut für Eisenforschung, 4 Düsseldorf, Max-Planck-Strasse 1, West Germany.

†Armco Steel Corporation, Research and Technology, Middletown, OH 45043, U.S.A.

other conduction and diffusion problems with moving phase boundary. The superiority of the Green's function method compared to the conventional numerical procedure is caused by the transformation of the partial differential equation for heat flow into an integral equation which has to be solved at the boundaries only. By this measure the difficulties associated with stability and convergence are avoided, and the computer time is decreased. The formulation has been performed in the following for the case of melting of a porous sphere in its own melt. So the melting temperatures are the same for the shell and the porous region. The treatment includes that for the melting of dense spheres in which the frozen shell and initial sphere have the same material constants. The numerical results will be mostly for iron. With little effort the equations can be modified for the case in which the shell and original sphere have different melting points, e.g. for melting of a metal sphere in a slag medium.

EXPLANATION OF MODEL AND MATHEMATICAL FORMULATION OF THE MELTING PROBLEM

The porous metal sphere of temperature T_{0s} and radius R_0 is submersed (e.g. by electromagnetic force) at time $t = 0$ into an infinite medium of liquid metal at temperature T_{0m}. Figure 1 shows the temperature as a function of distance r for the initial period when a solid shell is present. The temperature gradient is discontinuous at $r = R_0$ because of the different heat conductivities in the porous domain and the dense shell. After some time growth stops and afterwards the radius R decreases. At time $t = t_a$ the dense shell has disappeared again, and subsequently the porous domain is melted. The governing equations are the following:

Porous region I during time $t < t_a$:

$$\frac{\partial T}{\partial t} - \alpha_{\mathrm{I}}\left(\frac{\partial^2 T}{\partial r^2} + \frac{2}{r}\frac{\partial T}{\partial r}\right) = 0, \quad 0 < r < R_0 \tag{1}$$

$$\frac{\partial T}{\partial r} = 0, \quad r = 0 \tag{1a}$$

$$\left.\begin{aligned} T &= T_{0s}, \quad r < R_0, \\ T &= T_f, \quad r = R_0, \end{aligned}\right\} \quad t = 0. \tag{1b}$$

Dense region II during time $t < t_a$:

$$\frac{\partial T}{\partial t} - \alpha_{\mathrm{II}}\left(\frac{\partial^2 T}{\partial r^2} + \frac{2}{r}\frac{\partial T}{\partial r}\right) = 0, \quad R_0 < r < R \tag{2}$$

$$T = T_f, \quad r = R \tag{2a}$$

$$\lambda_{\mathrm{II}}\frac{\partial T}{\partial r} - h(T_{0m} - T_f) = \frac{\mathrm{d}R}{\mathrm{d}t}\rho_{\mathrm{II}}\Delta H, \quad r = R \tag{2b}$$

$$R = R_0, \quad t = 0. \tag{2c}$$

Both systems of differential equations are coupled by the expressions

$$T_{\mathrm{I},R_0} = T_{\mathrm{II},R_0}, \tag{3a}$$

$$\lambda_{\mathrm{I}}\left(\frac{\partial T}{\partial r}\right)_{\mathrm{I},R_0} = \lambda_{\mathrm{II}}\left(\frac{\partial T}{\partial r}\right)_{\mathrm{II},R_0} \tag{3b}$$

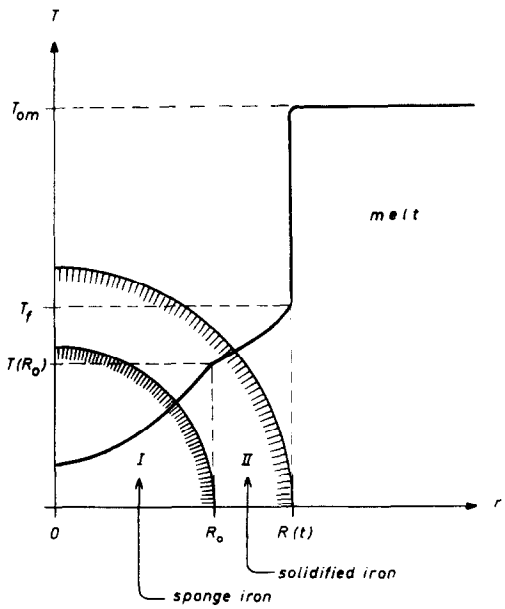

FIG. 1. Description of heat flow problem.

Equations (1) and (2) are Fourier's law of heat conduction in media with constant temperature diffusivity and equations (1a), (1b) and (2a)–(2c) are the corresponding boundary and initial conditions. Equation (2b) represents the heat balance at the melt–solid interface. The coupling equations (3a) and (3b) are statements to the fact that the temperature and heat flux are continuous at $r = R_0$. The melting temperature T_f is taken to be constant, that is formation of an additional mushy zone (occurring in melting and freezing of alloys) and mass transfer are not considered.

When the dense shell is remelted at $t = t_a$, the sphere is present again with its original radius R_0 and the temperature profile is that obtained by solution of equations (1)–(3). For $t > t_a$, only equation (1) has to be solved within the domain $0 < r < R(t) < R_0$ with the following boundary and initial conditions:

Porous region during time $t > t_a$:

$$\frac{\partial T}{\partial r} = 0, \quad r = 0, \tag{4a}$$

$$T = T_f, \quad r = R, \tag{4b}$$

$$\lambda_{\mathrm{I}}\frac{\partial T}{\partial r} - h(T_{0m} - T_f) = \frac{\mathrm{d}R}{\mathrm{d}t}\rho_{\mathrm{I}}\Delta H, \quad r = R, \tag{4c}$$

$$R = R_0, \quad t = t_a, \tag{4d}$$

$$T(r, t_a) = T_a(r), \quad 0 < r < R_0, \quad t = t_a. \tag{4e}$$

If the shell has the same material properties as the original body, (e.g. if a dense iron sphere is submersed into liquid iron) the problem simplifies. In this case $\alpha_{\mathrm{I}} = \alpha_{\mathrm{II}}$, $\lambda_{\mathrm{I}} = \lambda_{\mathrm{II}}$, $\rho_{\mathrm{I}} = \rho_{\mathrm{II}}$, and for the total range of time equation (2) is solved by using the boundary and initial conditions (1a), (1b), (2a)–(2c).

Equations (1)–(4) are transformed into dimensionless forms by defining:

$$U = \frac{T - T_f}{T_f - T_{0s}}, \tag{5a}$$

$$p = \frac{t\alpha_{\mathrm{I}}}{R_0^2}, \tag{5b}$$

$$s = \frac{r}{R_0}, \tag{5c}$$

$$S = \frac{R}{R_0}. \tag{5d}$$

By this measure the usual advantage of decreasing the number of variables is obtained. Moreover, the additional advantage of defining U in the form of equation (5a) is that U becomes zero at the melt/solid interface and that, consequently, some of the integrals cancel in the integral equation presented in the subsequent section. Incorporating (5a)–(5d) into (1)–(4) the following equations result.

Porous region I during time $p < p_a$:

$$\frac{\partial U}{\partial p} - \left(\frac{\partial^2 U}{\partial s^2} + \frac{2}{s}\frac{\partial U}{\partial s}\right) = 0, \quad 0 < s < 1, \tag{6}$$

$$\frac{\partial U}{\partial s} = 0, \quad s = 0, \tag{6a}$$

$$\left.\begin{aligned} U &= -1 \quad s < 1 \\ U &= 0 \quad\ \ s = 1 \end{aligned}\right\} \quad p = 0. \tag{6b}$$

Dense region II during time $p < p_a$:

$$\frac{\partial U}{\partial p} - \frac{\alpha_{\mathrm{II}}}{\alpha_{\mathrm{I}}}\left(\frac{\partial^2 U}{\partial s^2} + \frac{2}{s}\frac{\partial U}{\partial s}\right) = 0, \quad 1 < s < S, \tag{7}$$

$$U = 0, \quad s = S, \tag{7a}$$

$$\frac{\partial U}{\partial s} - Bi_{\mathrm{II}} U_{0m} = \frac{\mathrm{d}S}{\mathrm{d}p} Ph_{\mathrm{II}}, \quad s = S, \tag{7b}$$

$$S = 1, \quad p = 0 \tag{7c}$$

$$Bi_{\mathrm{II}} = \frac{hR_0}{\lambda_{\mathrm{II}}}, \tag{7d}$$

$$Ph_{\mathrm{II}} = \frac{\alpha_{\mathrm{I}}}{\alpha_{\mathrm{II}}} \frac{\Delta H}{c_{\mathrm{II}}(T_f - T_{0s})} \tag{7e}$$

$$U_{\mathrm{I},s=1} = U_{\mathrm{II},s=1} \tag{8a}$$

$$\left(\frac{\partial U}{\partial s}\right)_{\mathrm{I},s=1} = \frac{\lambda_{\mathrm{II}}}{\lambda_{\mathrm{I}}}\left(\frac{\partial U}{\partial s}\right)_{\mathrm{II},s=1} \tag{8b}$$

For time $p > p_a$ equation (6) is applicable and the boundary conditions are:

Porous region during time $p > p_a$:

$$\frac{\partial U}{\partial s} = 0, \quad s = 0, \tag{9a}$$

$$U = 0, \quad s = S, \tag{9b}$$

$$\frac{\partial U}{\partial s} - Bi_{\mathrm{I}} U_{0m} = \frac{\mathrm{d}S}{\mathrm{d}p} Ph_{\mathrm{I}}, \quad s = S, \tag{9c}$$

$$S = 1, \quad p = p_a, \tag{9d}$$

$$U(s, p_a) = U_a(s), \quad s < 1, \quad p = p_a, \tag{9e}$$

$$Bi_{\mathrm{I}} = \frac{hR_0}{\lambda_{\mathrm{I}}}, \tag{9f}$$

$$Ph_{\mathrm{I}} = \frac{\Delta H}{c_{\mathrm{I}}(T_f - T_{0s})}. \tag{9g}$$

It is noticed that the Biot numbers Bi_{I} and Bi_{II} are present only in the form of the product with U_{0m}. Hence, these products can be used as modified Biot numbers.

$$Bi'_{\mathrm{I}} = Bi_{\mathrm{I}} U_{0m}, \tag{9h}$$

$$Bi'_{\mathrm{II}} = Bi_{\mathrm{II}} U_{0m}. \tag{9i}$$

From equations (7d), (9f) and (7e), (9g) it follows that $\lambda_{\mathrm{I}}/\lambda_{\mathrm{II}} = Bi_{\mathrm{II}}/Bi_{\mathrm{I}}$ and that $\alpha_{\mathrm{I}}/\alpha_{\mathrm{II}} = (Ph_{\mathrm{II}} c_{\mathrm{II}})/(Ph_{\mathrm{I}} c_{\mathrm{I}})$. Since for the considered problem $c_{\mathrm{I}} = c_{\mathrm{II}}$, $\alpha_{\mathrm{I}}/\alpha_{\mathrm{II}} = Ph_{\mathrm{II}}/Ph_{\mathrm{I}}$. Consequently the dimensionless radius is a function of solely five dimensionless quantities, namely the variable p, and the constants Bi'_{I}, Bi'_{II}, Ph_{I}, Ph_{II}.

INTEGRAL FORMULATION

In order to derive the integral equations for this system we introduce a Green's function

$$G(s, p; \xi, \tau) = \frac{1}{8\pi s\xi\sqrt{[\pi\beta(p-\tau)]}}\left\{\exp\left[-\frac{(s-\xi)^2}{4\beta(p-\tau)}\right] - \exp\left[-\frac{(s+\xi)^2}{4\beta(p-\tau)}\right]\right\} \tag{10}$$

which has zero gradient at $s = 0$ and vanishes at $s = \infty$ and for which

$$\int_0^\infty 4\pi\xi^2 G \,\mathrm{d}\xi = 1, \quad \int_0^\infty 4\pi s^2 G \,\mathrm{d}s = 1.$$

The equation (10) gives the temperature present at radius s and time p when an instantaneous spherical heat source of unit strength operates at $s = \xi$ and $p = \tau$. G satisfies the heat-conduction equation

$$\beta\left(\frac{\partial^2 G}{\partial s^2} + \frac{2}{s}\frac{\partial G}{\partial s}\right) - \frac{\partial G}{\partial p} = -\frac{\delta(s-\xi)\,\delta(p-\tau)}{4\pi s\xi}. \tag{11}$$

The constant β is equal either to 1 or $\alpha_{\mathrm{II}}/\alpha_{\mathrm{I}}$ depending on the domain (I or II) to which equation (10) is applied. The Green's function also satisfies its adjoint equation in the (dimensionless) source coordinates ξ, τ which, after a small positive value ε is added to the time p to avoid the singularity for $\tau = p$, can be written as

$$\beta\left(\frac{\partial^2 G_1}{\partial \xi^2} + \frac{2}{\xi}\frac{\partial G_1}{\partial \xi}\right) + \frac{\partial G_1}{\partial \tau} = -\frac{\delta(s-\xi)\,\delta(p+\varepsilon-\tau)}{4\pi s\xi}. \tag{12}$$

The symbol $G_1(s, p; \xi, \tau) = G(s, p+\varepsilon; \xi, \tau)$ is introduced to distinguish from G appearing in equation (11). Similarly, the heat-conduction equation can be

written in the source coordinates

$$\beta\left(\frac{\partial^2 U}{\partial \xi^2}+\frac{2}{\xi}\frac{\partial U}{\partial \xi}\right)-\frac{\partial U}{\partial \tau}=0, \quad 0<\xi<S. \tag{13}$$

Multiplying (12) by U and equation (13) by G_1, subtracting from each other, and then integrating with respect to ξ and τ over the ξ, τ space with the upper limit $\xi=\xi(\tau=p)$, $\tau=p$, one obtains the integral equation

$$\int\int\frac{\partial(G_1 U)}{\partial \tau}4\pi\xi^2\,\mathrm{d}\xi\,\mathrm{d}\tau-\beta\int\int\left|\frac{\partial}{\partial \xi}\left(G_1\frac{\partial U}{\partial \xi}-U\frac{\partial G_1}{\partial \xi}\right)+\frac{2}{\xi}\left(G_1\frac{\partial U}{\partial \xi}-U\frac{\partial G_1}{\partial \xi}\right)\right|4\pi\xi^2\,\mathrm{d}\xi\,\mathrm{d}\tau$$
$$=\int\int\frac{U\,\delta(s-\xi)\,\delta(p+\varepsilon-\tau)}{4\pi s\xi}4\pi\xi^2\,\mathrm{d}\xi\,\mathrm{d}\tau=0. \tag{14}$$

By application of Green's theorem the area integral is converted into the line integral.

$$\int_l (UG_1)4\pi\xi^2\,\mathrm{d}\xi+\beta\int_l\left|G_1\frac{\partial U}{\partial \xi}-U\frac{\partial G_1}{\partial \xi}\right|4\pi\xi^2\,\mathrm{d}\tau=0. \tag{15}$$

Equation (15) is the starting equation for setting up the integral equations for the time $p<p_a$ during which a solidified shell is present, and for $p>p_a$ when the porous domain is melting. The contours over which the integration has to be performed is shown in Fig. 2.

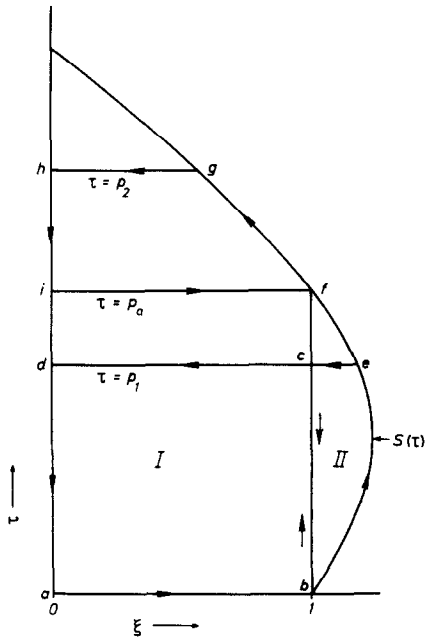

FIG. 2. Integration contour for equation (15).

Porous region I

For time $p<p_a$ (e.g. $p=p_1$ in Fig. 2) the equation for the porous region is obtained by integrating along the line extending from $\xi=0/\tau=0$ (point a) over $\xi=1/\tau=0$ (point b) over $\xi=1/\tau=p$ (point c) over $\xi=0/\tau=p$ (point d) to $\xi=0/\tau=0$ (point a). After taking the limit $\varepsilon\to 0$ and by the use of

$$\lim_{\varepsilon\to 0}4\pi\int_0^1(G_1U)_{\tau=p}\xi^2\,\mathrm{d}\xi=U(s,p), \tag{16}$$

we obtain with $G=G_1$ for $\beta=1$ and with the boundary and initial conditions (6a) and (6b)

$$U(s,p)=\int_0^p\left(G_1\frac{\partial U}{\partial \xi}\right)_{1,\xi=1}4\pi\xi^2\,\mathrm{d}\tau-\int_0^p\left(U\frac{\partial G_1}{\partial \xi}\right)_{1,\xi=1}4\pi\xi^2\,\mathrm{d}\tau-\int_0^1 G_{1,\tau=0}4\pi\xi^2\,\mathrm{d}\xi. \tag{17}$$

For the dense shell integration is along the line extending from $\xi=1/\tau=0$ (point b) over $\xi=S/\tau=p$ (point e) over $\xi=1/\tau=p$ (point c) to $\xi=1/\tau=0$ (point b). With

$$\lim_{\varepsilon\to 0}4\pi\int_1^{S(\tau=p)}(UG_1)_{\tau=p}\xi^2\,\mathrm{d}\xi=U(s,p) \tag{16a}$$

and using $G=G_{II}$ for $\beta=\alpha_{II}/\alpha_I$ and boundary conditions (7a), (7b), (8a), (8b) we obtain:

Dense region II

$$U(s,p)=\frac{\alpha_{II}}{\alpha_I}\int_0^p\left|G_{II}\left(Ph_{II}\frac{\mathrm{d}S}{\mathrm{d}\tau}+Bi''_{II}\right)\right|_{\xi=S}4\pi\xi^2\,\mathrm{d}\tau-\frac{\alpha_{II}}{\alpha_I}\int_0^p\frac{\lambda_I}{\lambda_{II}}G_{II}\left(\frac{\partial U}{\partial \xi}\right)_{1,\xi=1}4\pi\xi^2\,\mathrm{d}\tau+\frac{\alpha_{II}}{\alpha_I}\int_0^p\left(U\frac{\partial G_{II}}{\partial \xi}\right)_{\xi=1}4\pi\xi^2\,\mathrm{d}\tau. \tag{18}$$

Porous region for $p>p_a$

For the time $p>p_a$ (e.g. $p=p_2$ in Fig. 2) integration is along the line connecting the points $\xi=0/\tau=p_a$ (point i), $\xi=1/\tau=p_a$ (point f), $\xi=S/\tau=p$ (point g), $\xi=0/\tau=p$ (point h), $\xi=0/\tau=p_a$ (point i) in Fig. 2 with

$$\lim_{\varepsilon\to 0}4\pi\int_0^{S(\tau=p)}(UG_1)_{\tau=p}\xi^2\,\mathrm{d}\xi=U(s,p) \tag{16b}$$

and equation (9a) to (9g) yielding

$$U(s,p)=\int_{p_a}^p\left|G_I\left(Ph_I\frac{\mathrm{d}S}{\mathrm{d}\tau}+Bi'_I\right)\right|_{\xi=S}4\pi\xi^2\,\mathrm{d}\tau+\int_0^1(G_IU)_{\tau=p_a}4\pi\xi^2\,\mathrm{d}\xi. \tag{19}$$

Equations (17), (18) and (19) express the temperature at any value of s and p in terms of temperature and temperature gradient at the boundaries $s=1$ and $s=S$. This is the advantage of the integral formulation since the problem of heat conduction inside of the sphere is reduced to one involving only the spherical surfaces of the domains.

Equations (17)–(19) have to be applied in the following to the surfaces at $s=1$ and $s=S$. In order to avoid the singularities arising when $\xi=S$, the points are considered inside of the domains but infinitesimally close to the boundaries. At such points temperature and gradient can be set equal to the values

exactly at the boundaries without introducing significant error.

Equations (17) and (18) contain $dS/d\tau$, the temperature and the temperature gradient at $s = 1$, and equation (19) $dS/d\tau$ and $U_a(s)$ as unknown quantities. The evaluation of the integral is only possible numerically, and the technique used for that will be described in the Appendix.

COMPARISON OF NUMERICAL RESULTS WITH ANALYTICAL SOLUTIONS AVAILABLE FOR CERTAIN LIMITING CASES

It should be expected that the growth rate of the sphere at $t = 0$ should coincide with that at a planar surface. For zero superheat ($T_{0m} = T_f$) the analytical equation

$$\frac{\sqrt{k}}{2} Ph_{II} \sqrt{\pi} \exp \frac{k}{4}\left(\operatorname{erf}\frac{\sqrt{k}}{2} + \frac{\lambda_{II}}{\lambda_I}\sqrt{\frac{\alpha_I}{\alpha_{II}}}\right) = \frac{\alpha_I}{\alpha_{II}} \quad (20)$$

is valid in which k is the (dimensionless) parabolic rate constant given by

$$k = \frac{(S-1)^2}{p}\frac{\alpha_I}{\alpha_{II}}. \quad (20a)$$

Table 1. Constants used in the numerical computations

	Sponge iron	Dense iron
ΔH (cal g^{-1})	66.25	66.25
ρ (g cm^{-3})	2.6	7.65
c (cal g^{-1} °C^{-1})	0.196	0.196
α (cm^2 s^{-1})	0.01	0.06
λ (cal °C^{-1} cm^{-1} s^{-1})	0.0051	0.09
T_f (°C)	1536	1536
h (cal cm^{-2} °C^{-1} s^{-1})*	0.6	0.6

*Heat-transfer coefficient valid for $R_0 = 1$ cm.

Numerical calculations were performed with the material constants known for sponge iron and dense iron (Table 1). The results as plotted in Fig. 3 show that the growth rate becomes parabolic and identical to that calculated with (20) as time approaches zero. It can be proved by further derivations that expression (20) is indeed the exact solution of equations (17) and (18) for $t \to 0$. For $t \to \infty$ the value of R has to approach a limiting value R_{max}. R_{max} is calculated from a heat balance in which the heat necessary for heating the initial sphere to melting temperature is set equal to that liberated by solidification.

$$\left(\frac{R_{max}}{R_0}\right)^3 = 1 + \frac{\rho_I c_I (T_f - T_{0s})}{\Delta H \rho_{II}}. \quad (21)$$

Other limiting cases for which the computer results can be checked include those for which the heat conductivities are ∞ in region I and II, or 0 in region I. For $\lambda_I = \lambda_{II} = \infty$ the sphere is heating up instantaneously after immersion to the melting temperature. The heat necessary for this is taken out of the melt, causing an instantaneous growth from R_0 to R_{max} given by equation (21). The subsequent decrease of radius is represented by

$$R = R_{max} - \left[\frac{h(T_{0m} - T_f)}{\Delta H \rho_{II}}\right] t \quad \text{for} \quad t < t_{E,II} \quad (22)$$

and

$$R = R_0 - \left[\frac{h(T_{0m} - T_f)}{\Delta H \rho_I}\right](t - t_{E,II}) \quad \text{for} \quad t > t_{E,II} \quad (23)$$

where $t_{E,II}$ is the time at which region II has disappeared

$$t_{E,II} = \frac{(R_{max} - R_0)\Delta H \rho_{II}}{h(T_{0m} - T_f)}. \quad (24)$$

For $\lambda_I = 0$ there is no initial growth of shell. Each layer is first heated from T_{0s} to T_f before it is melting. Consequently the heat flux from the melt to the surface of the sphere $h(T_{0m} - T_f)$ is balanced by $dR/dt[(T_f - T_{0s})\rho_I c_I + \rho_I \Delta H]$ and the decrease of radius is given by

$$R = R_0 - \left[\frac{h(T_{0m} - T_f)}{(T_f - T_{0s})\rho_I c_I + \rho_I \Delta H}\right] t. \quad (25)$$

The results obtained by numerical solution of equations (17)–(19) approach nicely to those given by equations (22) and (23), or (25) respectively, when the heat conductivities are increased to very high or decreased to very low values (Figs. 4 and 5).

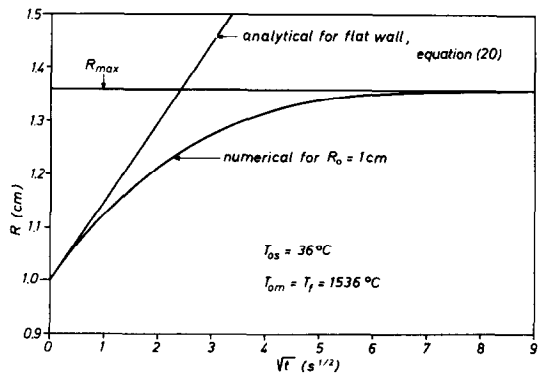

FIG. 3. Growth of a sponge iron pellet submerged in liquid iron of melting temperature (material properties see Table 1).

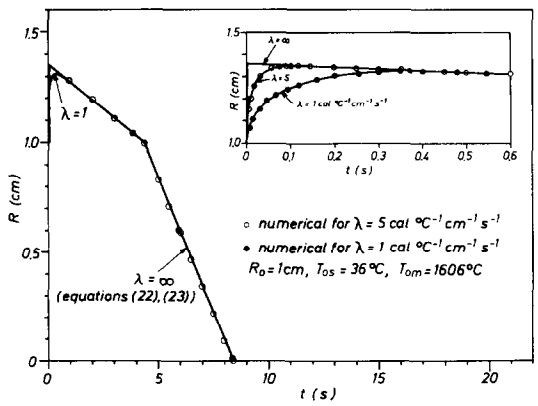

FIG. 4. Numerical results for melting behavior of a sphere when the heat conductivities ($\lambda_I = \lambda_{II}$) are very high, and limiting case for $\lambda_I = \lambda_{II} = \infty$. Numerical values of constants used see Table 1.

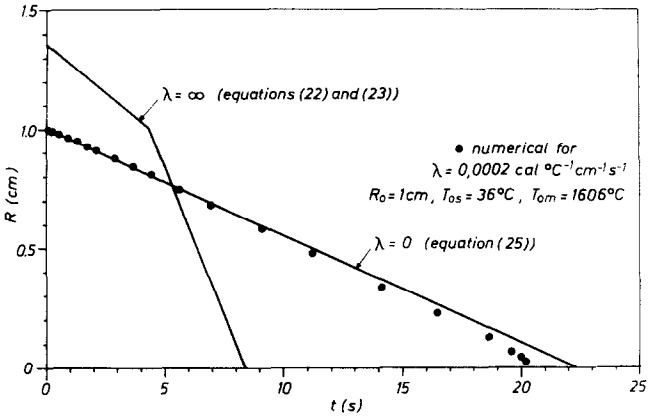

FIG. 5. Numerical results for melting behavior of a sphere when the heat conductivities ($\lambda_I = \lambda_{II}$) are very small, and limiting case for $\lambda_I = 0$. Numerical values of constants used see Table 1. The limiting case $\lambda_I = \lambda_{II} = \infty$ is shown for comparison ($R_0 = 1$ cm, $T_{0s} = 36$°C, $T_{0m} = 1606$°C).

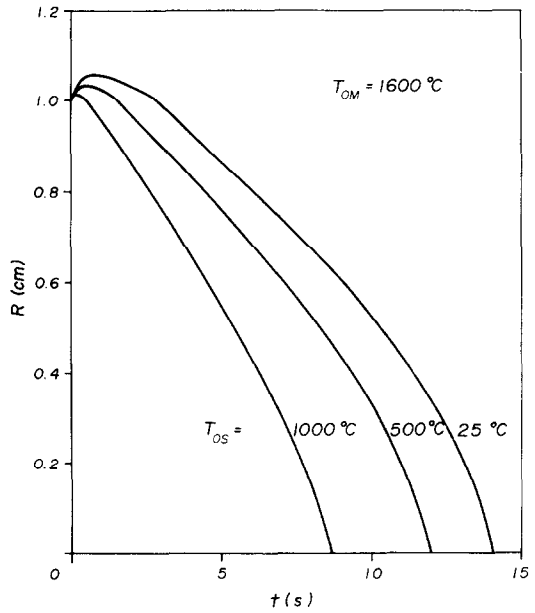

FIG. 6. Melting behavior of sponge iron pellets with $R_0 = 1$ cm as a function of initial pellet temperature T_{0s} for $T_{0m} = 1600$°C. Numerical values of constants used see Table 1.

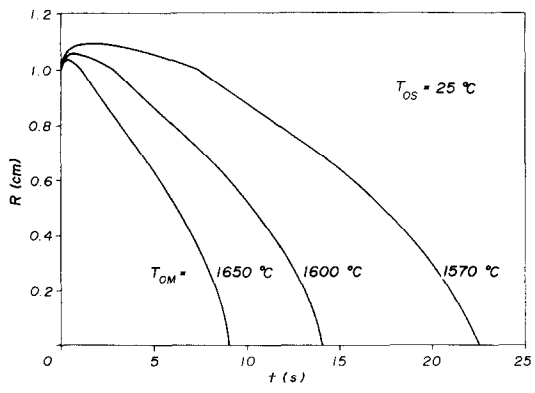

FIG. 7. Melting behavior of sponge iron pellets with $R_0 = 1$ cm as a function of the temperature of iron melt T_{0m} for $T_{0s} = 25$°C. Numerical values of constants used see Table 1.

NUMERICAL RESULTS

The numerical results as calculated with equations (17)–(19) are presented in the following. The change of radius with time for a sponge iron sphere immersed in liquid iron (material properties as given in Table 1) is shown in Fig. 6 for selected values of starting temperature T_{0s}. In Fig. 7 the similar curves are given illustrating the influence of superheat. As might be expected the maximum thickness of the solidified shell and the total melting time increase with the decrease of T_{0s} and T_{0m}. It is also seen that the region II is present only during a comparatively short period.

It is of interest to investigate the extent with which the shell formation is influenced by the difference of material properties used for regions I and II. Additional computations were performed for the hypothetical case that the layer II has the material properties of the pellet. Further, the R–t curve was calculated for melting of the dense iron sphere. The results are shown in Fig. 8. If the lower values of heat conductivity and density are used for the shell (curve b) the maximum thickness and life of the shell becomes somewhat smaller compared to the values obtained with the material properties for dense iron (curve a). The total melting time t_E, however, is the same within limits of precision of the calculation. The behavior is drastically different for a dense sphere (curve c). The shell grows to a much larger thickness and is present for a considerably longer time than in the melting of pellets.

Extensive additional calculations were carried out to obtain values for the total melting time of dense spheres ($\alpha_I = \alpha_{II}$, $\rho_I = \rho_{II}$, $\lambda_I = \lambda_{II}$). Since only equation (17) has to be solved, calculations are much less involved and require comparatively small computer time. The dimensionless melting time $p_E = t_E \alpha / R_0^2$ is a function solely of the two other dimensionless variables Bi' and Ph. The obtained relationship between these quantities is shown in Fig. 9. For each value of Ph the calculated curves approach the limiting lines valid for $\lambda \to \infty$ at low Bi', and for $\lambda \to 0$ at high Bi'. The equations valid for the limiting cases can be easily

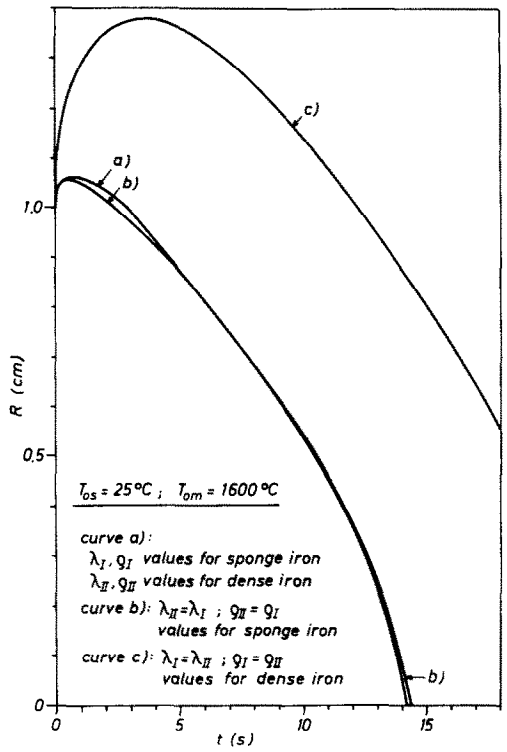

FIG. 8. Results of the computations for the case that the same material properties are used for domains I and II, (curves b and c) in comparison to those obtained with different material properties (curve a).

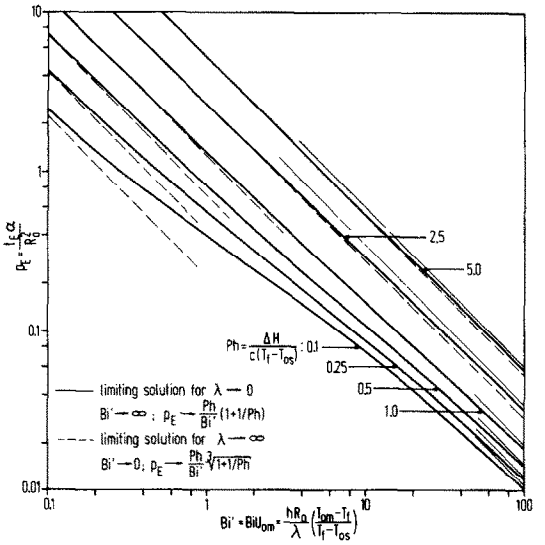

FIG. 9. Dimensionless melting time p_E of spheres submerged into their own melt as a function of modified Biot number Bi' and Ph number.

deduced from (21) and (22) or from (25), respectively

$$\lim_{\lambda \to \infty} p_E = \frac{Ph}{Bi'} \sqrt[3]{\left(1 + \frac{1}{Ph}\right)}, \tag{26}$$

$$\lim_{\lambda \to 0} p_E = \frac{Ph}{Bi'} \left(1 + \frac{1}{Ph}\right). \tag{27}$$

From the curves in Fig. 9 the melting time of any dense metal sphere can be easily obtained for many conditions. The graph is also applicable to a close approximation to the melting of sponge iron pellets, since (see Fig. 8) little error of t_E is caused in the range considered here if the shell properties ϱ_{II}, λ_{II}, α_{II} are set equal to those of the initial pellet.

CONCLUDING REMARKS

In the present paper the melting rate of metal spheres which were immersed into their own liquid was calculated. Initially, the solid shell freezes around the sphere which first grows and then melts again. The shell is dense and has different material properties from the porous region. The heat flow equation is solved for both domains by application of the Green's function technique.

The numerical results are given for the melting rate of sponge iron pellets in liquid iron as a function of the preheat temperature of the pellet and the superheat of the melt. Additional computations were performed for the case when the shell has the same material properties as the original sphere. These computations are simpler and involve less computer time because the heat flow equation has to be solved only for one single domain. It is shown that the total melting time of the pellets as computed with the simplified procedure (using the properties of the pellet also for the shell) is practically identical to that obtained by solution of the problem for the two domains. The dimensionless total melting time is calculated for a wide range of conditions and the results are presented as a function of Biot and phase conversion numbers.

In the present computations the melting point is taken to be a constant. Hence, the results are valid for the melting of pure metals. The theory may also be applied, however, to a close approximation, to the melting of low alloyed metals with small freezing range, e.g. the melting of low carbon sponge iron in low carbon liquid steel.

REFERENCES

1. P. B. Grimado and B. A. Boley, Numerical solution for the symmetric melting of spheres, *Int. J. Num. Meth. Engng* **2**, 175–188 (1970).
2. R. Jeschar and P. Busch, Theoretische Untersuchungen des Abschmelzverhaltens einer Einzelkugel und von Haufwerken im Hinblick auf das Einschmelzen von Eisenschwamm, Bericht 1/74, Institut für Wärmetechnik und Industrieofenbau der Technischen Universität Clausthal (1974).
3. R. I. Pedroso and G. A. Domoto, Perturbation solution for spherical solidification of saturated liquids, *J. Heat Transfer* 7, 42–46 (1973).
4. J. George and P. S. Damle, On the numerical solidification for spherical free boundary problems, *Int. J. Num. Meth. Engng* **9**(1), 239–245 (1975).
5. C.-L. Huang and Y.-P. Shih, A perturbation method for spherical and cylindrical solidification, *Chem. Engng Sci.* **30**, 897–906 (1975).
6. K. Stephan, Schmelzen und Erstarren geometrisch einfacher Körper, *Kältetechnik-Klimatisierung* **23**(2), 42–46 (1971).
7. J. F. Elliott and J. D. Naumann, Liquid silicates as media for heat transfer, in *Metal–Slag–Gas Reactions and Processes*, pp. 238–250, The Electrochem. Soc., London, (1975).

8. H. A. Friedrichs, H. Jauer, O. Knacke, Zur Auflösung eines Kristalls in der eigenen Schmelze, *Z. Metallkde* **63**, 169–172 (1972).
9. Y.-K. Chuang and J. Szekely, On the use of Green's function for solving melting or solidification problems, *Int. J. Heat Mass Transfer* **14**, 1285–1294 (1971).
10. Y.-K. Chuang, W. Wepner and K. Schwerdtfeger, Berechnung der interdendritischen Anreicherung von Kohlenstoff und Sauerstoff bei der Erstarrung von Stahl, *Arch. Eisenhüttenwes.* **44**, 243–250 (1973).
11. Y.-K. Chuang and O. Ehrich, On the integral technique for spherical growth problems, *Int. J. Heat Mass Transfer* **17**, 945–953 (1974).

APPENDIX

Numerical Solution of Integral Equations (17), (18), (19)

The time scale is divided into intervals by the nodes, $p_0, p_1, p_2, \ldots, p_n, \ldots, p_N$, where $p_0 = 0$ and $p_N = p$. Within each interval dS/dp, temperature and temperature gradient at the surface of region I are taken to be constant, and the integration can be performed analytically between the limits of the interval. Finally the total integral is obtained by summation.

Region I ($0 < s < 1$) at $p < p_a$ [equation (17)]:

$$U(s, p_N) = \sum_{n=1}^{N} \left(\frac{\partial U}{\partial s}(p_m)\right)_{I,s=1} \int_{p_{n-1}}^{p_n} G_{I,\xi=1}\, 4\pi\xi^2\, d\tau - \sum_{n=1}^{N} U(p_m)_{s=1} \int_{p_{n-1}}^{p_n} \left(\frac{\partial G_I}{\partial \xi}\right)_{\xi=1} 4\pi\xi^2\, d\tau - \int_0^1 G_{I,\tau=0}\, 4\pi\xi^2\, d\xi. \tag{A1}$$

Region II ($1 < s < S$) at $p < p_a$ [equation (18)]:

$$U(s, p_N) = \frac{\alpha_{II}}{\alpha_I} \sum_{n=1}^{N} \left[Ph_{II} \frac{dS}{dp}(p_m) + Bi''_{II} \right] \int_{p_{n-1}}^{p_n} G_{II,\xi=S}\, 4\pi\xi^2\, d\tau - \frac{\alpha_{II}\lambda_I}{\alpha_I\lambda_{II}} \sum_{n=1}^{N} \left[\frac{\partial U}{\partial s}(p_m) \right]_{I,s=1} \int_{p_{n-1}}^{p_n} G_{II,\xi=1}\, 4\pi\xi^2\, d\tau + \frac{\alpha_{II}}{\alpha_I} \sum_{1}^{N} U(p_m)_{s=1} \int_{p_{n-1}}^{p_n} \left(\frac{\partial G_{II}}{\partial \xi}\right)_{\xi=1} 4\pi\xi^2\, d\tau. \tag{A2}$$

The time p_m is some value between p_{n-1} and p_n, and can be set equal to $(p_{n-1}+p_n)/2$, or to p_{n-1}, or to p_n if the interval is sufficiently small.

Region I at $p > p_a$ [equation (19)]:

$$U(s, p_n) = \sum_{n=n(p_a)}^{N} \left[Ph_I \frac{dS}{dp}(p_m) + Bi''_I \right] \int_{p_{n-1}}^{p_n} G_{I,\xi=S}\, 4\pi\xi^2\, d\tau + \sum_{l=1}^{M} \left[\frac{U(p_a)_{l-1} + U(p_a)_l}{2} \right] \times \int_{s_{l-1}}^{s_l} G_{I,\tau=p_a}\, 4\pi\xi^2\, d\xi. \tag{A3}$$

Here, l specifies the node on the s scale.

In order to obtain dS/dp for a value of p in the range $p < p_a$ equation (A1) is applied at the surface of region I. The calculation is started with $N = 1$. By setting $U(1, p_N)$ equal to $U(1, p_{N-1})$ [LHS of equation (A1)] and $U(p_m)$ also equal to $U(1, p_{N-1})$ a value is obtained for $[(\partial U/\partial s)(p_m)]_{I,s=1}$. With this value and using again $U(1, p_N) = U(1, p_{N-1}) = U(p_m)$, $(dS/dp)(p_m)$ is calculated with equation (A2) at $s = S$. With known values of $(dS/dp)(p_m)$ and $(\partial U/\partial s)(p_m)$, $U(1, p_N)$ is computed by application of equation (A2) at $s = 1$. An alternative procedure would be to apply both equations (A1) and (A2) at $s = 1$ and set their LHS equal. With $U(p_m) = U(1, p_{N-1})$ an equation is generated containing $[(\partial U/\partial s)(p_m)]_{I,s=1}$ and $(dS/dp)(p_m)$ as unknown quantities. A second equation with the same unknown quantities is obtained by application of equation (A2) at $s = S$. Other possibilities exist, e.g. both equations (A1) and (A2) might be used inside of the domains at $1 \pm \Delta s$ to generate additional equations for $(\partial U/\partial s)(p_m)_{I,s=1}$. Iteration procedures can be applied at each interval to reach complete consistency of the various equations and, thereby, the highest desired accuracy. The computational procedure is particularly simple for $p > p_a$, or in the whole range of time if melting of a non-porous sphere is considered, because $(dS/dp)(p_m)$ is obtained by solving one single equation (equation A3) at $s = S$.

Most of the integrals contained in equations (A1)–(A3) have been solved in a previous publication. For the sake of completeness all of them are listed below.

Analytical solution of the integrals, appearing in equations (A1)–(A3):

$$\int 4\pi\xi^2 G_{\xi=1}\, d\tau = -\frac{1}{2\sqrt{\pi\beta s}} \left\{ \exp\left[-\frac{(s-1)^2}{y^2} \right] y + (s-1)E\left(\frac{s-1}{y}\right) - \exp\left[-\frac{(s+1)^2}{y^2} \right] y - (s+1)E\left(\frac{s+1}{y}\right) \right\} + C$$

$$\int 4\pi\xi^2 \left(\frac{\partial G}{\partial \xi}\right)_{\xi=1} d\tau = \frac{1}{2\beta} \left\{ E\left(\frac{s-1}{y}\right) + \frac{y}{\sqrt{\pi s}} \left(\exp\left[-\frac{(1-s)^2}{y^2} \right] - \exp\left[-\frac{(1+s)^2}{y^2} \right] \right) \right\} + C$$

$$\int 4\pi\xi^2 G_{\tau=0}\, d\xi = 0.5 \left\{ E\left(\frac{s+\xi}{y'}\right) - E\left(\frac{s-\xi}{y'}\right) + \frac{y'}{\sqrt{\pi s}} \left(\exp\left[-\frac{(\xi+s)^2}{y'^2} \right] - \exp\left[-\frac{(\xi-s)^2}{y'^2} \right] \right) \right\} + C$$

$$\int 4\pi\xi^2 G_{\xi=S}\, d\tau = \frac{H^2}{8\beta s} \left\{ E(z_1)\left(\tfrac{1}{2} - \frac{S}{H}\right) + E(z_2)\exp\left(-\frac{4A}{H}\right)\left(\tfrac{1}{2} - \frac{S}{H} + \frac{2A}{H}\right) - E(z_3)\left(\tfrac{1}{2} + \frac{S}{H}\right) - E(z_4)\exp\left(-\frac{4B}{H}\right)\left(\tfrac{1}{2} + \frac{S}{H} + \frac{2B}{H}\right) - \frac{2y}{\sqrt{\pi H}} \left[\exp(-z_1^2) - \exp(-z_3^2) \right] \right\} + C.$$

G is the Green's function in equation (10), and:

$$V_n = \frac{S_n - S_{n-1}}{p_n - p_{n-1}}$$

$$H = \frac{4\beta}{V_n}$$

$$A = -V_n(p - p_{n-1}) - S_{n-1} + s$$

$$B = -V_n(p - p_{n-1}) - S_{n-1} - s$$

$$y = \sqrt{[4\beta(p-\tau)]}$$

$$z_1 = \frac{y}{H} + \frac{A}{y}$$

$$z_2 = \frac{y}{H} - \frac{A}{y}$$

$$z_3 = \frac{y}{H} + \frac{B}{y}$$

$$z_4 = \frac{y}{H} - \frac{B}{y}$$

$$y' = \sqrt{(4\beta p)}.$$

LA FUSION DE SPHERES METALLIQUES AYANT DES ENVELOPPES INITIALEMENT GELEES AVEC DIFFERENTES PROPRIETES MATERIELLES

Résumé—La méthode des fonctions de Green est utilisée dans le calcul de la vitesse de fusion de sphéres métalliques poreuses. Ce probléme concerne de nouveaux procédés industriels, par exemple la fusion de billes de fer poreuses. Après immersion dans le métal liquide la coque gèle initialement autour de la sphère. La coque est dense et possède des propriétés matérielles différentes de celles de la région poreuse. L'équation de départ est la seconde loi de Fourier avec les conditions initiale et aux limites correspondantes. On montre, par utilisation des fonctions de Green, que les équations aux dérivées partielles pour les deux domaines peuvent être transformées en équations intégrales contenant seulement la température et les gradients de température à la surface du domaine et que, de cette façon, l'effort numérique est considérablement réduit. Les mêmes calculs sont conduits pour le problème plus simple de la sphère et de l'enveloppe ayant les mêmes propriétés. Dans ce cas, le temps adimensionnel de fusion totale est une fonction de deux autres groupements sans dimension et la relation fonctionnelle calculée est donnée pour un domaine d'intérêt pratique.

DAS ABSCHMELZEN VON METALLKUGELN UNTER BERÜCKSICHTIGUNG DER VERSCHIEDENEN MATERIALEIGENSCHAFTEN DER ANFÄNGLICH ANFRIERENDEN SCHALE

Zusammenfassung—Im vorliegenden Bericht wird die Abschmelzrate von porösen Metallkugeln berechnet, die in ihre eigene Schmelze eingetaucht werden. Zu Beginn friert eine feste Schale um die Kugel an, welche zuerst wächst und dann wieder abschmilzt. Die Schale ist im Gegensatz zum Kern nicht porös und besitzt andere Materialeigenschaften. Die Wärmeleitungsgleichung wird für beide Regionen durch Anwendung der Green'schen Methode gelöst.

Die numerischen Ergebnisse für die Abschmelzrate von Eisenschwammpellets in flüssigem Eisen werden als Funktion der Anfangstemperatur der Pellets und der Überhitzung der Schmelze angegeben. Weitere Rechnungen wurden für den Fall gleicher Stoffkonstanten von angefrorener Schale und ursprünglicher Kugel durchgeführt. Diese Rechnungen sind einfacher und benötigen weniger Computerzeit, weil die Wärmeleitungsgleichung nur in einer einzigen Region zu lösen ist. Die dimensionslose Abschmelzzeit ist über einen weiten Bereich von Bedingungen berechnet worden. Die Ergebnisse sind als Funktion der Biot- und Phasenübergangszahl dargestellt worden.

In den vorliegenden Rechnungen ist der Schmelzpunkt als konstant angenommen. Die Ergebnisse sind deshalb nur für reine Metalle gültig. Die Theorie kann jedoch in guter Näherung für das Abschmelzen von niedrig legierten Metallen mit geringem Erstarrungsintervall benutzt werden, z.B. auch für das Einschmelzen von schwach kohlenstoffhaltigem Eisenschwamm.

ПЛАВЛЕНИЕ МЕТАЛЛИЧЕСКИХ СФЕР С ЗАМЕРЗШИМИ ОБОЛОЧКАМИ, ОБЛАДАЮЩИМИ СВОЙСТВАМИ, ОТЛИЧНЫМИ ОТ СВОЙСТВ МАТЕРИАЛА СФЕРЫ

Аннотация — Для численного расчета скорости плавления пористых металлических сфер использовалась функция Грина. Эта проблема представляет интерес для новых промышленных процессов, например, при плавлении пористых железных окатышей. После помещения в жидкий металл оболочка вокруг сферы замерзает. Оболочка плотная и ее свойства отличаются от свойств пористой среды. Исходным уравнением является второй закон Фурье с соответствующими начальными и граничными условиями. Показано, что с помощью функции Грина дифференциальное уравнение в частных производных для теплового потока в двух расчетных областях может быть преобразовано в интегральные уравнения, включающие только температуру и градиенты температуры на поверхности области, что занчительно облегчает расчет. Такие же расчеты выполнены для более простой задачи, когда сфера и замерзшая оболочка имеют одинаковые свойства. В этом случае безразмерное общее время плавления является функцией только двух других безразмерных величин. Приводится расчетная функциональная зависимость, представляющая интерес для практического применения.